Combination of Deflection, Scattering/Extinction and Diffraction Measurements for the Analysis of Soot Particle Temperature, Size and Shape

B.Mandel and B.Ineichen

I.C. Engines and Combustion Technology Laboratory
Swiss Federal Institute of Technology
ETH-Zentrum, CH-8092 Zurich
Switzerland

ABSTRACT

The determination of soot particle size and shape in a diffusion flame is an important step on the way to understand soot particle origin and growth. Laser light scatter transmission method of G. Mie's theory have been used to study the behavior of soot particle diameter, number and density in steady and non-steady flames. Accurately determination of the *temperature dependent optical constant of soot particles* in flames is an substantial part of the diameter measurement.

Two strategies, one using an opto-acoustic laser beam deflection technique to measure the *soot temperature* and a light scattering/polarization extinction ratio method to measure the *refractive index, size* and *shape* were examined.

The technique called *opto-acoustic laser-beam deflection* was introduced to measure the local temperature in a diffusion flame close to a soot particle. Absorption of a 8-ns duration, 532 nm pulse from a frequency-doubled Nd:YAG laser by the soot particles, and subsequent local heating of the gas, produces an acoustic pulse deflecting two parallel HeNe-laser beams, which are detected by position sensing diodes. The comparison of the two diode signals (Fig. 2) delivers the acoustic velocity at the measurement point. To determine the local temperature belonging to the measured acoustic velocity a model was developed to consider the local equivalence ratio at the measurement point.

The change in optical properties and the change in soot particle characteristics are determined by the scattering/polarization extinction ratio method and the transmission/attenuation coefficient factor ratio method. In a first step scattering measurements at different laser wavelengths and polarization states deliver an information about the complex refractive index of the particles. The combination with transmission measurements and computed results of the Mie theory allows the determination of particle diameter. The influence of non-spherical particles will be investigated by a measurement of the diffraction pitch factor.

The experimental verification of the scattering/transmission method for particle size measurements in flames will be presented, and the properties of this technique to combustion diagnostic will be discussed.

INTRODUCTION

Determination of size and shape of particulates in chemically reacting systems such as flames or liquid fuel jet systems can be used to predict not only their growth and oxidation but also the radiative heat transfer from flame systems.

The techniques used for particle-size measurements in a flame system can be divided into two categories: *ex situ* and *in situ*. Extracting the particles from the flame by a mechanical probe or a water-cooled plate introduces other sizing techniques, such as electron microscopy. These *ex situ* techniques has been criticized because the flame is disturbed during sampling, and therefore the morphology of the extracted particles can be different from that of the primary particles in the flame.

For *in situ* particle-size measurements optical techniques are used with the advantages of non-intrusion of the flame and real-time analysis. Soot particle sizing in flames (1-6) utilizes the average scattered light intensity as a function of the wavelength and scattering direction.

The methods based on G. Mie's light scatter theory have made it possible to measure with some accuracy the diameter, number and density of soot particles in steady and non-steady diffusion flames. However, the optical constant of soot particles is an uncertain element in determining their diameter. A soot particle is an absorptive substance, its chemical composition is unclear, it changes in lifetime, and moreover its optical constant differs with the temperature of the soot particle. It is very difficult to determine accurately the complex *temperature dependent refractive index* (the optical constant). The temperature measurement of soot particles is an important foundation of the determination of the refractive index.

The existence of spherical particles is a strong requirement for the use of the Mie theory (7-10) to reduce the data. Nevertheless, in combustion systems, as it has been pointed out by several investigators (11-15), the particles after their formation depart from sphericity because of coalescence and subsequent agglomeration into non-spherical aggregates. The aggregates may have various shapes such as clusters, straight chains and / or random structures. The knowledge of the number of primary particles

that constitute the agglomerate, their largest dimension, as well as the refractive indices and the size of the primary particle represents the first step for a detailed characterization of a given agglomerate. In addition, since in general the aggregates are elongated structures with different largest dimensions, their aspect ration distribution needs to be determined, and when their total mass is required the number density must also be known.

In 1977, Eckbreth showed that laser-modulated incandescence from soot particles in a flame could easily overwhelm signals from Raman measurements, and he related the time dependence of this interference to laser heating, heat transfer to the medium, particle vaporization, and indirectly to the particle size (16). Greenhalgh has observed resonant CARS signals generated from C_2 molecules vaporized by pulsed lasers used to generate the CARS signal (17), and Dasch has studied the flame perturbations caused by vaporization of soot (18). However, the refractive index has long been estimated by measuring the energy reflecting power or by theoretical equations of dispersion models. Most typically, Senftleben et al. (19) actually measured the index within a visual region by using the highly accurate Drude's method. Dalzell et al. (20) made the soot pellets with acetylene and propane gas flames, and obtained the index by measuring the reflected energy and by calculations based on a dispersion model. Nevertheless, it is necessary to develop and establish a method of simultaneously measuring the diameter of soot particles, their temperature and complex refractive index in a non-contact way. This study has established a method for measuring both of them.

TEMPERATURE MEASUREMENT TECHNIQUE

Basic Considerations

The investigation of soot particle growth and oxidation is the main goal of this project. A slit burner, producing a two-dimensional flame, is the source of small particles. An analyzation of the scattered intensities under two different directions delivers the diameter of the particle.

The following part describes a new method to determine the flame temperature very close to a particle called opto-acoustic beam deflection (21). The knowledge of the refractive index, which depends strongly on this particle temperature, is the main problem in particle sizing techniques.

$$a = \sqrt{\kappa RT} \tag{1}$$

Our experimental technique is based on the thermodynamic dependence of the acoustic wave velocity form the temperature (Eq. 1). We implemented an experimental technique to measure in a first step the acoustic wave velocity in a gas, e.g., in a flame. The experimental arrangement is shown in Fig. 1. The computation of the specific heat of the gas at the measurement volume delivers, together with the experimental result of the acoustic wave velocity, the temperature T (Eq. 2).

The relationship between the temperature and the acoustic-wave propagation velocity is given by

$$T = a^2 \frac{M}{R(1 + R/c_v)} \tag{2}$$

where M is the molecular weight of the gas between the two measurement beams of the HeNe-laser.

The effective molecular weight and the specific heat of the mixture of intermediate combustion species are usually not known. However, the fuel-air flame in the experimental conditions of the present study does not change significantly during combustion. Therefore, the present opto-acoustic deflection temperatures can be calculated on the assumption that the thermodynamic parameters (specific heat) do not change over a wide range of temperature; this will be discussed in more detail in Section "Modeling".

The flame temperature T_f can be determined from the acoustic velocities in the flame a_f and air a_a and air temperature T_a by

$$\frac{T_f}{T_a} = \left(\frac{a_f}{a_a}\right)^2 \tag{3}$$

Under the assumption that the radiation of the soot particles produces a negligible drop in temperature relative to that of the surrounding gas, Eq. 3 can be used. If the gas velocity is still compared to the speed of sound, Eq. 4 can be written as

$$\frac{T_f}{T_a} = \left(\frac{\Delta t_a}{\Delta t_f}\right)^2 \tag{4}$$

Therefore a comparison of the relative transit times in the flame Δt_f and in air Δt_a delivers the temperature T.

Apparatus

Temperature Measurement By Opto-acoustic Laser Beam Deflection The first step for the measurement of the temperature T in a flame, belonging to the description of the opto-acoustic beam deflection described in Chapter "Basic Considerations" demands the determination of the acoustic wave velocity of the gas at the measurement volume. The experimental setup is shown in Fig. 1.

Two parallel beams from a Melles He-Ne laser intersected the Nd:YAG laser beam inside the flame. The two He-Ne laser beams were focused in the flame using long-focal-length lenses (typically 500 mm). The beam diameter near the focal point was less then 1 mm. A small wire which was hitted by a mildly focused frequency-doubled Nd:YAG laser (8 nsec pulse length, 200 mJ energy at 532 nm) was used as the acoustic source. A localized heating, produced by absorption of the pump beam by the target, acts to heat the surrounding gases and increases pressure. This acoustic pulse propagates through the flame, causing a change in the refractive index of the medium. The observation of the deflection of one beam delivers an information about the arrival of the acoustic pulse at that beam. Two probe beams separated by 4 mm were used to monitor the sound velocity.

The two He-Ne laser beams were arranged in such a way that no significant perturbation of the flame would be produced by the wire at the position of the probe beams. Two position-sensitive detectors, each having four quadrants, were used to monitor the deflection of the probe beams. The two quadrants of the diodes oriented in the direction of the deflection were used in the experiments after making sure that the other two quadrants having nearly

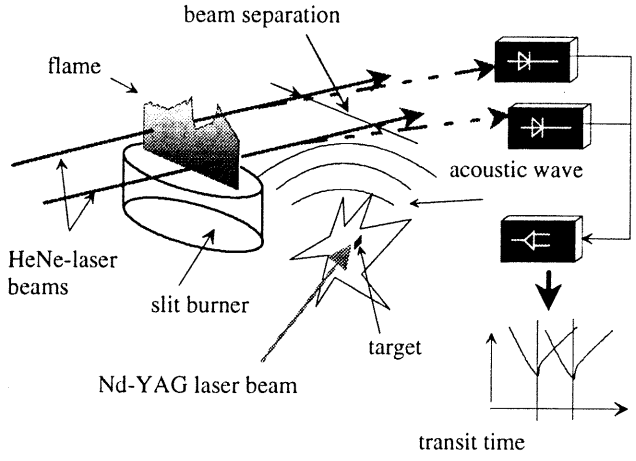

Fig. 1 Experimental setup for the opto-acoustic laser beam deflection

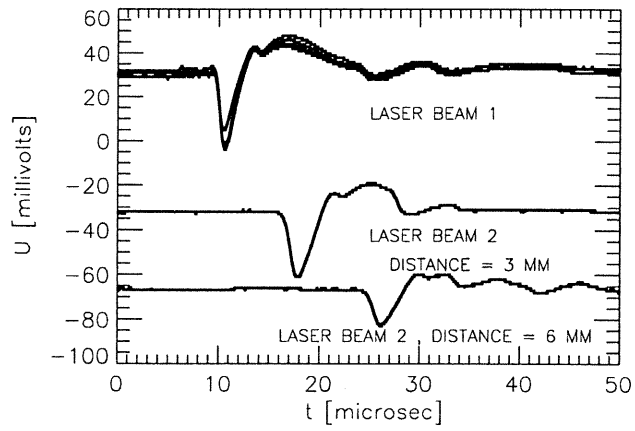

Fig. 2 Multiple deflection signals at the same measurement volume.

no deflection signals. The signals from the individual quadrants were passed through amplifiers to change the photo currents into voltages and then to main amplifiers. Electronic filtering surpressed low-frequency signal fluctuations caused by flame turbulence. The signal shape was observed on a LeCroy model 9410 oscilloscope and triggered by the Q-switch pulse from the Nd:YAG laser. The deflections were digitized with 6.66 nsec resolution and a single deflection was used to determine the transit time. It was not necessary to average the deflection signals in order to obtain signals with good SNRs as shown in Fig. 2.

Measurement

Adjustment of opto-acoustic laser beam deflection

To assess the usefulness of the results two critical geometric parameters of the setup were analyzed. In a first step the distance between the two parallel probe beams was optimized to a value of s = 4 mm with an accuracy of Δs = +/- 0.02 mm using a diffraction technique with circular apertures. The distance between the source of the acoustic wave and the first probe beam was optimized and carefully adjusted. A target outside of the plane defined by the two HeNe probe beams would result in a deflection which contains an imbalance between the two quadrants perpendicular to the main direction of the deflection.

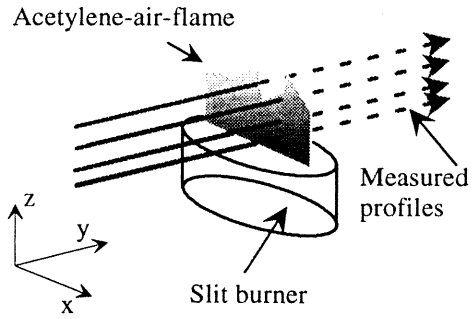

Fig. 3 Traces of the measured profiles

A flame with an adjusted, pre-mixed equivalence ratio of λ = 0.7 was used to identify temperature profiles in the y-z-plane (the thickness-height-plane) through the flame in different heights above the burner exit plane. Fig. 3 shows the trace of the measured profiles. Each profile contains approximately 15 measurement points along the y-axis, where 5 measurements were made by each point. The statistical deviation was less than 1% by measuring the transit time in the flame (Fig. 2). The exact y-position of the profiles is defined by the focal plane of the two HeNe laser beams.

Modeling

A model, delivering the correct calculation of the thermodynamic parameters, like specific heat c_v, forms the background of the temperature measurement.

Local Jet Velocity In The Flame Fig. 3 shows the coordinates used to describe the velocity field. The velocity components u,v,w, belonging to these coordinates, are determined as derivatives of the potential ϕ. The assumption of an incompressible fluid (22) (ρ = cons.) changes the continuity equation to

$$\frac{\partial u}{\partial x}+\frac{\partial v}{\partial y}+\frac{\partial w}{\partial z}=0 \qquad (5)$$

Using the definition of the potential ϕ together with Eq. 5 yields Eq. 6, which must be solved under the boundary conditions ($u_\infty = 0$).

$$\frac{\partial^2\phi}{\partial x^2}+\frac{\partial^2\phi}{\partial y^2}+\frac{\partial^2\phi}{\partial z^2}=0 \qquad (6)$$

The momentum equation Eq. 7

$$u\frac{\partial u}{\partial x}+v\frac{\partial u}{\partial y}=\nu\frac{\partial^2 u}{\partial y^2} \qquad (7)$$

and

$$\frac{\partial u}{\partial x}+\frac{\partial v}{\partial y}=0 \qquad (8)$$

yield the solution of the problem. Figure 4 shows the velocity profile u through the flame for different equivalence ratios λ between 0.5 and 0.9.

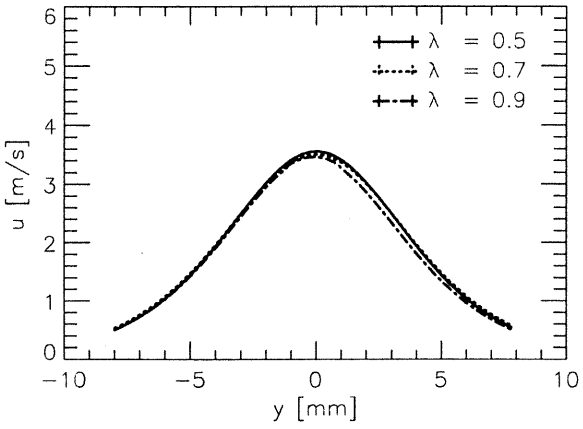

Fig. 4 Local computed velocity profiles for different pre-mixed flames, at 45 mm above the burner exit plane

Determination of local stoichiometry After determination of the local velocity field in the flame, it is possible to gain the local stoechiometry as a function of the adjusted, pre-mixed equivalence ratio λ_{global}. The fuel mass concentration c_F yields (22) under the assumption of Schmidt = 1

$$u\frac{\partial c_F}{\partial x}+v\frac{\partial c_F}{\partial y}=\nu\frac{\partial^2 c_F}{\partial y^2} \qquad (9)$$

This equation is similar to the momentum equation (Eq. 7) which leads to a linear relationship between fuel mass concentration c_F and velocity u .With the boundary condition $c_\infty = 0$ and the fuel mass preservation we find the solution for the local stoechiometry λ_{local} as

$$\lambda_{local}=0.21\frac{n_A}{n_F}=0.21\frac{1-c_F}{c_F}\frac{M_F}{M_A} \qquad (10)$$

where n are the molecular numbers and M are the molecular weights of air and fuel.
The profiles of the local stoechiometry, corresponding to the local velocity profiles u, are shown in Fig. 5.

Use of the CHEMKIN code for the determination of the temperature The CHEMKIN code (23) was used to calculate the ratio of the given species C, CO, CO_2, H_2O ,H_2 and OH in the burned region of the flame. With this code, it is possible to calculate an equilibrium for a reaction for given species and to gain the estimated temperature for this reaction in a state of equilibrium. The species-dependent viscosity μ of the different components was also considered. One of the calculated profiles is shown in the Fig. 6.

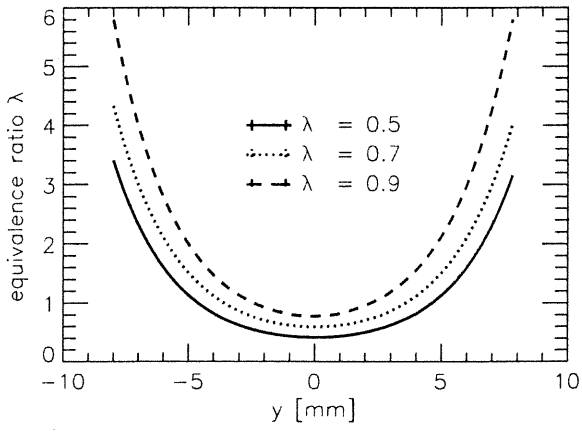

Fig. 5 Local computed equivalence ratio λ for different pre-mixed flames, at 45 mm above the burner exit plane

Results

Fig. 6 shows measured temperature profiles in a flame with a global pre-mixed equivalence ratio of λ = 0.7. The model leads to profiles with a local minimum in the center of the profiles between two high peaks, corresponding to the calculated profiles in Fig. 8.

For a flame with a global equivalence ratio of λ_{global} = 0.7, the measurements in different heights of the same flame were compared with holographic interferometry, another established method for temperature measurements (Fig. 7).

Comparison of theoretical investigations with measurement results provides evidence for the usefulness of the measurement method. Fig. 8 shows temperature profiles for a λ = 0.7 at a height of h = 20 mm above the burner exit plane, compared with the corresponding modeling results.

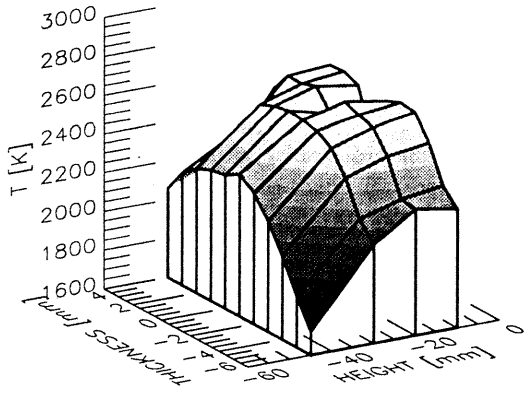

Fig. 6 Measured temperature profiles in different heights above the burner exit plane for a global equivalence ratio of $\lambda_{global} = 0.7$

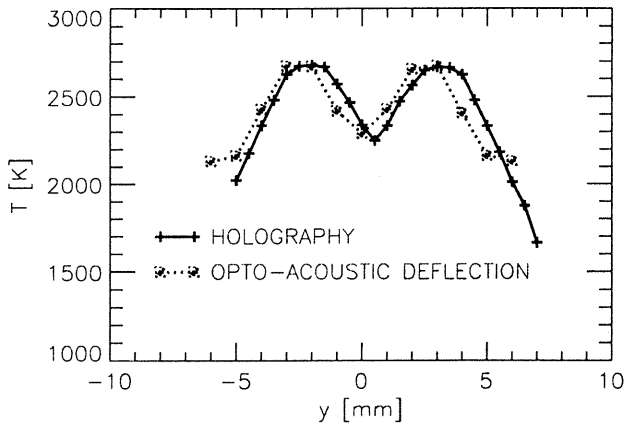

Fig. 7 Measured temperature profiles at 20 mm above the burner exit plane; comparison of holography and opto-acoustic laser beam deflection

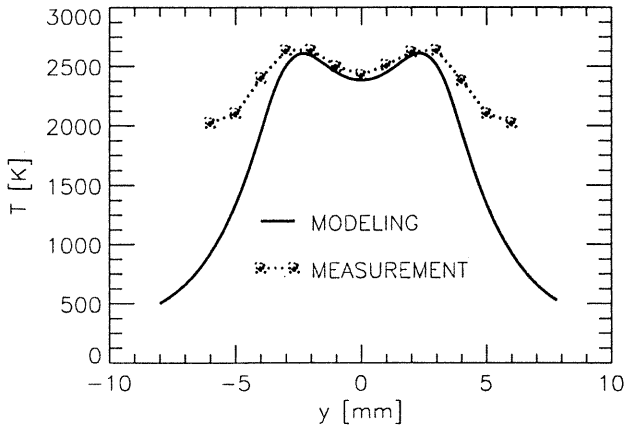

Fig. 8 Temperature profiles for $\lambda = 0.7$ at a height of h = 20 mm

PARTICLE SIZE MEASUREMENTS

Part I of this paper shows some promise for particle size measurements. Investigations of individual temperature of particles has been reported. This makes the determination of the refractive index and therefore the particle size measurements sensitive to the particle size and the exact shape of the particle.

Many optical measurement technique have been developed, the most commonly used methods measure the time histories of either the size of individual particles that pass through a single point in space (e.g. phase-Doppler anemometry (24)) or size distributions of many particles contained within a laser sheet (25). Providing accurate, instantaneous particle size distributions, neither method is capable.

Obtaining spatial resolution imaging techniques are required ranging from photography to holography to measurements of scattered intensities. Photography and holography are restricted to particles larger than approximately 10 μm and to relatively small numbers of particles. Scattered intensity measurements are constrained to systems of spherical particles because of the use of Lorenz-Mie theory in determining particle size.

This paper describes the ability of polarization ratio extinction method. The advantage of the technique is that they do not require calibration with known size particles and in order to obtain size information the temperature dependent refractive index can be measured as partially shown in Part I of this paper.

Scattering from a single, spherical particle illuminated by a plane wave propagating through the surrounding medium is described by the Lorenz-Mie theory. One can show that the scattering amplitudes in the far field are linearly related to the incident field with the components of the scattered and incident fields polarized parallel and perpendicular to the scattering plane. In case of a linearly polarized incident field the scattered field will be in general elliptically polarized, however if the incident field is polarized either perpendicular or parallel to the scattered plane, the scattered field retains the same linear polarization with respect to the scattering plane. If the incident light is polarized parallel, the scattered light will be parallel polarized however, the off axis collected scattered rays will have a small fraction of their power not completely perpendicular polarized to the scattering planes.

Limitations of accuracy

Several factors should be considered; first, one is supposedly attempting to measure the local size distribution; second, the incoherent summation is only valid if the scattering from a large number of particles falls on a single detector. If only a small number of particles is present, the result can be biased by a single large particle or by coherent interference with laser illumination. The polarization ratio method is applicable for size determination since the scattered light arising from the perpendicular incident

polarization scales roughly as D^2 in the 5 - 100 µm diameter range.

The advantage of measuring the polarization ratio lies in the fact that it is a relative measurement of the scattering of the same particle. Furthermore, through the measurement of the polarization extinction ratio we can determine experimentally the refractive index which has to be well known or else errors will occur in the particle size determination. If the particle size is known, the polarization extinction ratio can be used to determine for instance the particle temperature.

The technique is in general more tolerant of other particles between the collection lens and the scattering particle, because near forward scattering does not significantly change polarization properties.

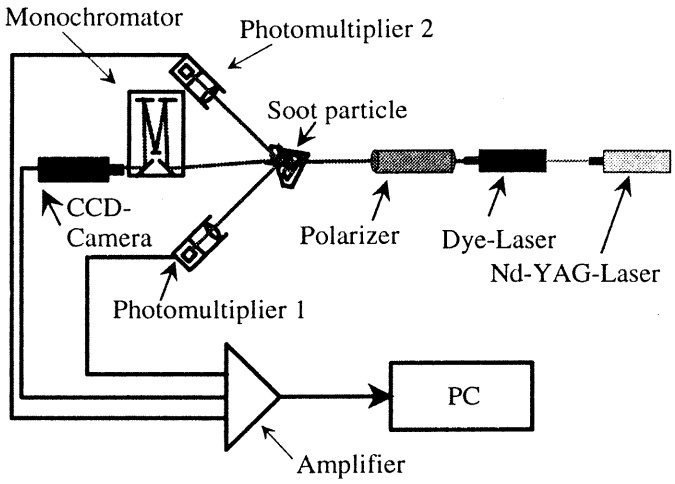

Fig. 9 Experimental setup for the particle size measurement

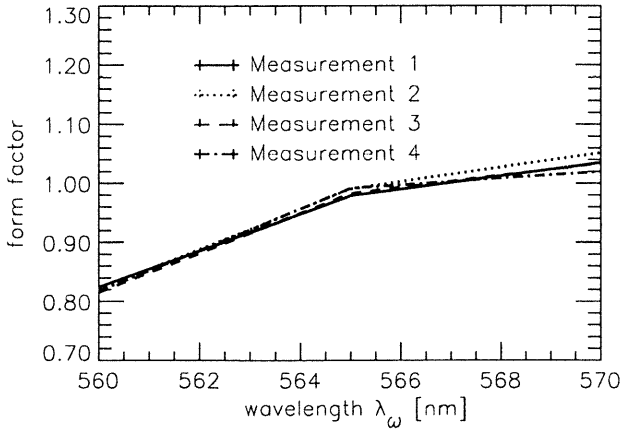

Fig. 10 Intensity ratio under two angles for different wavelengths, scattered at a diffuser

Experimental setup

The experimental setup is illustrated in Fig. 9. The output of a Nd:YAG frequency doubled pumped broadband dye laser is polarized at 45° and is focused to a width of approximately 400 µm into the slit burner. The polarization components had a 100:1 extinction ratio. Pulsed energy and pulse width were approximately 15 mJ at 10 ns.

Fig. 10 shows the wavelength dependence on the form factor determined by measurement of the scattered light under two angles (θ = 30° and θ = 60°). This is an agreement with the theory described above.

CONCLUSIONS

The method used in this study delivers easy reproducible and consistent results for temperature profile measurement in a flame environment with a high resolution and single-shot detection. The acoustic deflection method is relatively simple to implement and was subjected to preliminary experimental tests, but measurements of soot heating are yet to be performed. Preliminary experimental results for the scattered intensities make us believe, that the described method will allow us to determine the optical constant as a first step in particle sizing.

NOMENCLATURE

a	=	acoustic velocity, m/s
c	=	mass concentration, -
c_v	=	specific heat, J/(g K)
h	=	height above the burner head, mm
m	=	mass, kg
M	=	molecular weight, g/mole
n	=	refractive index, -
R	=	universal gas constant, 8.3143 J/mole K
s	=	beam separation, mm
t	=	transit time of the acoustic wave, s
T	=	temperature, K
u	=	velocity component belonging to x, m/s
v	=	velocity component belonging to y, m/s
w	=	velocity component belonging to z, m/s
x	=	coordinate parallel to the flame, mm
y	=	coordinate perpendicular through the flame ("thickness"), mm
z	=	coordinate perpendicular to the flame ("height"), mm
λ	=	stoechiometry of the flame, -
λ_ω	=	wavelength of an electromagnetic wave, nm
ϕ	=	fluid stream potential
ρ	=	fluid density, kg/m^3
μ	=	fluid viscosity, Ns/m^2

Subscripts

a	=	air
f	=	flame
F	=	fuel
global	=	condition of the gas before ignition
local	=	condition in the burning flame
v	=	constant volume

ACKNOWLEDGMENTS

The authors wish to thank Prof. M. K. Eberle for his encouragement; and are grateful to K. Boulouchos for helpful discussions. P. Obrecht, Obrecht Engineering wrote the software for experimental process control, data acquisition and data evolution. Special thanks to T. Steiner for his help in the modeling. We also wish to thank P. Eberli, S. Nguyen-Chi and A. Schmid for the technical support.
Financial support for the current work was provided by the Swiss Federal Office of Energy (BEW), Grant Nr. EF-FOS (89)004.

REFERENCES

1. Erickson, W.D., Williams, D.C. and Hottel, H.C., 1964. *Light scattering measurements on soot in a benzene-air flame*, Combust. Flame **8**, 127.

2. Kunugi, M. and Jinno, H., 1966. *Determination of size and concentration of soot particles in diffusion flames by a light scattering technique*, 11th Symp. (Int.) on Combust. 257.

3. Dalzell, W.H., Williams, W.H. and Hottel, H.C., 1970. Measurements, Combust. Flame **14**, 161.

4. D'Alessio, A., et al., 1972., *Optical and chemical investigations on fuel-rich methane-oxygen premixed flames at atmospheric pressure*, 14th Symp. (Int.) on Combust. p. 941.

5. Magnussen, B.F., 1975. *An investigation into the behavior of soot in a turbulent free jet C_2H_2-flame*, 15th Symp. (Int.) on Combust. p. 1415.

6. D'Alessio, A., et al., 1975. *Soot formation in methane-oxygen flames*, 15th Symp. (Int.) on Combust. p. 1427.

7. Mie, G., 1908. *Beitrage zue Optik trüber Medien speziell kolloidaler Metallosungen*, Ann. Phys. 25, 377.

8. Bohren, C.F. and Huffman, D.R., 1983. *Absorption and scattering of Light by Small Particles*, John Wiley, New York.

9. Van de Hulst, H.C., 1957. *Light Scattering by Small Particles*, John Wiley, New York.

10. Kerker, M.K, 1969. *The Scattering of Light and Other Electromagnetic Radiation*, Academic Press, New York.

11. Jones, A.R., 1972. *Scattering and emission of radiation by clouds of elongated particles*, J. Phys. D: Appl. Phys. D: Appl. Phys. 5, LI.

12. Lee, S.C. and Tien, C.L., 1983. *Effect of soot shape on soot radiation*, J. Quant. spectrosc. Radiat. Transfer 29 (3), 259.

13. Drolen, B.L. and Tien, C.L., 1986. *Absorption and scattering of agglomerated soot in flames*, Easter Section: Fall tech. Meet., The Combustion Institute.

14. Drolen, B.L. and Tien, C.L., 1987. *Absorption and scattering of agglomerated soot particulate*, J. Quant, Spectrosc. Radiat. Transfer 37, 433.

15. Mackowski, D.W., Alterkirch, R.A. and Mengüc, M.P., 1987. *Extinction and absorption coefficients of cylindrically-shaped soot particles*, Entral States Section: Spring tech. Meet., The Combustion Institute.

16. Eckbreth, A. C., 1977. *Effects of Laser-Modulated Particulate Incandescence on Raman Scattering Diagnostics*, J. Appl. Phys.**48**, 4473.

17. Greenhalgh, D. A., 1983. *RECLAS: Resonant-Enhanced CARS from C_2 Produced by Laser Ablation of Soot Particles*, Appl. Opt. **22**, 1128

18. Dasch, C., General Motors Research Center; private communication.

19. Senftleben, H. and Benedikt, E., 1918. Annalen der Physik, (IV)-54 65.

20. Dalzell, W. H. and Sarofim, A. F. , Transaction of the ASME, **91**-1, 100 (1969-2).

21. Ineichen, B., Mandel, B. and Steiner, T., Sept. 1992. *Soot particle detection and characterization in a diffusion flame*, 2nd Workshop on: "Fluid mechanics, combustion emissions and Reliability in Reciprocating Engines", Capri.

22. Thomann, H., 1986. *Strömungslehre I + II*, Manuscript zur Vorlesung Strömungslehre, ETHZ.

23. Kee, R. J., Miller, J. A. and Rupley, F. M., 1992. *CHEMKIN II: A Fortran Chemical Package for the Analysis for Gas Phase Chemical Kinetics*, Sandia Report: SAND-8009. UC-706, New Mexico and California

24. Bachalo, W. D. and Houser M. J., *Phase/Doppler spray analyzer for simultaneous measurement of drop size and velocity distributions*, Opt. Eng. **23**, 583-590 (1984)

25. Dodge, L. G., Rhodes, D. J. and Reitz, R. D., *Drop size measurement techniques for sprays*, Appl. Opt. **26**, 2144-2154 (1987)